Article
Journal of Hydrogels
Vol. 1, 1–7, 2014
www.aspbs.com/jh

Luminescent Hydrogel Composites Based on Y(III), Eu(III) and Tb(III) Complexes

Corneliu S. Stan*, Marcel Popa, and Cătălina A. Peptu

"Gheorghe Asachi" Technical University, Faculty of Chemical Engineering and Protection of the Environment, Department of Natural and Synthetic Polymers, 73, Bd. Prof. Dr. docent Dimitrie Mangeron, 700050 Iasi, Romania

Spherical shaped photoluminescent hydrogels were prepared by introduction of Y(III), Eu(III) and Tb(III) complexes with 2-(1H-1,2,4-Triazol-3-yl)pyridine as ligand, in spherical shaped poly(acrylamide-co-acrylic acid) potassium salt beads. The blue, green, red luminescence of the complexes and the dimensional characteristics of the prepared hydrogels were long term preserved by using small adds of glycerol during the swelling stage of the preparation process. Before embedment, the complexes prepared at 1/3 metal to ligand ratio were investigated through elemental chemical analysis, thermal analysis, FT-IR, and fluorescence spectroscopy while the obtained hydrogels composites were investigated through SEM and fluorescence spectroscopy. The remarkable emissive properties of the prepared hydrogels may recommend them as photoluminescent probes in various applications.

KEYWORDS: *Luminescent Hydrogels, Lanthanide Complexes, Yttrium Complexes.*

INTRODUCTION

Optical materials were always in the main area of research interest due to their various applications ranging from optics, optoelectronics to medical investigation techniques. In this context various lanthanide compounds became increasingly interesting for state of the art applications. Their characteristic narrow emission bands due to the radiative transitions within $4f$ orbitals[1,2] are barely affected by the molecular entities located in the vicinity of the luminescent center. Efficient radiative transitions within the shielded inner f orbitals, can be triggered by an adequate energy transfer from the surroundings to the emissive lanthanide center. One of the most convenient approaches is the complexation of the lanthanides with ligands able to efficiently harvest and further transfer the energy to the lanthanide luminescent center. A chromophore containing ligand which could complex the lanthanide cations may provide an efficient path for triggering the radiative transitions through an indirect "antenna effect" of the chromophore. The sensitization could be achieved directly by direct coordination of a chromophore to the central lanthanide cation. Although yttrium is not part of the lanthanide group, it's physical properties and chemical behavior are very similar[3] fact also sustained by the investigations performed in this work. Among various classes of ligands, carboxylates, polyaminocarboxylates, β-diketonates or pyrazole derived compounds,[2,4,5] succinimide and derivatives[6] were successfully used for obtaining photoluminescent lanthanide complexes. As obtained, many of the lanthanide complexes are not suitable for direct applications since a series of drawbacks (sensitivity to moisture, poor thermal stability, toxicity) may be quite limiting. These limitations could be addressed by embedding the complexes in various matrices. Besides decoupling the sensitive structure of the complexes from various environmental factors, the encapsulation may also provide the required compatibility with targeted applications. Among various approaches, lanthanide complexes were embedded in silica matrix[7] or in polymer matrices aiming optoelectronic[8] and bioimaging applications.[9] Hydrogel composites containing lanthanide compounds were reported as suitable materials especially for bioimaging applications. Thus, by using lanthanum salts, agar-carbomer hydrogel composites were prepared by microwave assisted co-polymerization and used as "*in vivo*" agents for medical analyses.[10] Various lanthanide complexes used as prepared or introduced in

*Author to whom correspondence should be addressed.
Email: stancs@tuiasi.ro
Received: 10 October 2013
Accepted: 14 July 2014

silica matrices were further encapsulated in hydrogels for detecting various organic compounds in water.[11, 12]

In this work red, green and blue photoluminescent hydrogel composites were prepared through embedment of new Eu(III), Tb(III) and Y(III) complexes with 2-(1H-1,2,4-Triazol-3-yl)pyridine in spherical shaped poly(acrylamide-co-acrylic acid) potassium salt beads. Prior to embedment, the complexes prepared at 1/3 metal to ligand ratio were investigated through elemental analysis, thermal analysis, FT-IR, fluorescence spectroscopy while the obtained hydrogel composite monoliths were supplementary investigated through SEM and fluorescence spectroscopy.

EXPERIMENTAL DETAILS

Materials

2-(1H-1,2,4-Triazol-3-yl)pyridine (97%) and poly(acrylamide-co-acrylic acid) potassium salt (1 mm diameter spherical shaped beads) were purchased from Sigma-Aldrich while Yttrium chloride ($YCl_3 \times H_2O$, 99,99%), Europium chloride ($EuCl_3 \times 6H_2O$, 99,9%) and Terbium chloride ($TbCl_3 \times 6H_2O$, 99,9%) were purchased from Alfa–Aesar. Absolute ethanol and high purity Milli-Q water were used for preparation and washing operations.

Preparation of Photoluminescent Hydrogel Composites

Prior to hydrogel composite obtaining, the $[TbL_3(H_2O)_3]$ $[EuL_3(H_2O)_3]$ and $[YL_3(H_2O)_3]$ free complexes were prepared. Firstly, aqueous solutions of terbium chloride, europium chloride yttrium chloride and 2-(1H-1,2,4-Triazol-3-yl)pyridine with concentrations corresponding to 1/3 metal to ligand were prepared by dissolving 1 mmol of each $TbCl_3 \times 6H_2O$, $EuCl_3 \times 6H_2O$ and $YCl_3 \times H_2O$ in 2 mL high purity water while three identical ligand solutions are prepared by dissolving 3 mmol of 2-(1H-1,2,4-Triazol-3-yl)pyridine (denoted as HL) in a mixture of 3 mL MiliQ water and 1 mL ethanol. The complexes were obtained by mixing each prepared ligand solution with the corresponding Y, Eu, Tb chloride solutions. The complexation reactions were performed at 40–45 °C under moderate stirring for about 120 minutes. For investigation purposes, the complexes were obtained in their solid crystalline form by using aprox. 1/3 of the prepared aqueous solutions which were first dried at room temperature and then at 60–70 °C, under vacuum, till constant weight. The rest of the aqueous solutions of prepared complexes (4 mL each) were used for the preparation of the hydrogel composites. Each of the complex aqueous solutions were mixed with 2 mL of glycerol and then soaked in aprox. 2 g Poly(acrylamide-co-acrylic acid) potassium salt beads. The process may take between 3 to 7 days till the entire mixture of aqueous complexes solutions and glycerol is swallowed (aprox. 0.66 mmol of complex in 2 g Poly(acrylamide-co-acrylic acid) potassium salt beads). At the end of the process the diameter of the spherical polymer matrix beads increase to more then 800%. For long term dimensional stabilization and for increasing the photoluminescent emission intensity the retained water is removed in an oven for 48–72 hours by heating at 40 °C under vacuum. The high boiling point of the retained glycerol prevents evaporation, therefore, the shape and dimensional characteristics of the hydrogel composite are long term preserved. After removal of the trapped water, the mean diameter of the composite spheres is stabilized at aprox. 500% compared with the initial polymer spheres prior to soaking operation. The prepared photoluminescent hydrogel composites are presented in Figure 1, each picture being taken under excitation with a 4 W UV-A Philips TL4WBLB fluorescent lamp with a 360–380 nm peak emission.

Characterization Techniques

For the free complexes investigation, elemental chemical analysis was performed on Thermo Fisher Scientific Flash EA-1112CHNS/O equipment provided with Eager 300 software. The IR spectra were recorded in the 4000–400 cm^{-1} range, using a Digilab FTS-2000 FT-IR spectrometer, according to KBr pellet method. The thermal stability was studied on a Mettler Toledo TGA-SDTA851e, under an airflow rate of 20 mL/min. The heating rate was adjusted at 10 °C/min in the 50–900 °C range. SEM micrographs were recorded with a Hitachi SU-1510 equipment, working at 30 KV accelerating voltage. The fluorescent emission and excitation spectra of free complexes and prepared hydrogel composites were recorded on a Horiba Fluoromax 4P provided with a powder analysis adapter.

RESULTS AND DISCUSSION

Prior to soaking in the polymer matrix the structure of the prepared complexes was investigated. The reaction involved in formation of the prepared photoluminescent complexes is presented in Figure 2. The coordination number of the Y^{3+}, Eu^{3+} and Tb^{3+} cations used for preparing the investigated complexes is 9 through the bidentate behavior of the 2-(1H-1,2,4-Triazol-3-yl)pyridine (HL) ligand and also by the participation of 3 water molecules direct coordinated at the central cation.[13–15]

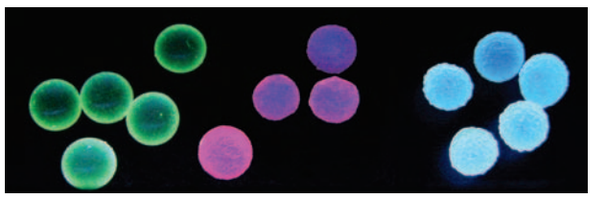

Figure 1. Prepared hydrogel composites with embedded (left to right) $[TbL_3(H_2O)_3]$, $[EuL_3(H_2O)_3]$ and $[YL_3(H_2O)_3]$ complexes under excitation with a UV-A fluorescent lamp.

Figure 2. Reaction involved in complexation of the Y^{3+}, Eu^{3+} and Tb^{3+} cations with the 2-(1H-1,2,4-Triazol-3-yl)pyridine ligand.

The proposed structure of the investigated complexes is sustained by the following presented investigations.

Elemental Chemical Analysis

Table I presents the recorded experimental results for the free complexes prior to soaking in the polymer matrix and also the calculated theoretical values. As could be noted, the recorded experimental results are in good concordance with the calculated values and also with the data obtained from thermal analysis (see below). The slightly higher values recorded for oxygen and hydrogen contents are most probably due to the small amounts of physical bonded water trapped in the structure.

Thermal Analysis

The thermal behavior of free complexes was evaluated, the results being presented in Table II. The decomposition parameters were provided by the accompanying software of the investigation equipment calculated by the generic methods as described here.[16] In the earlier stages, the decomposition of the free complexes are summarized by the following processes:

$$(M(L)_3(H_2O)_3)_{(s)} \xrightarrow{t\,^\circ C} (M(L)_3)_{(s)} + 3(H_2O)_{(g)} \quad \text{where } M = Y^{3+}, Eu^{3+}, Tb^{3+} \qquad (1)$$

$$(M(L)_3)_{(s)} \xrightarrow{t\,^\circ C} B_{(g)} + M_2O_{3(s)} \quad \text{where B are volatiles} \qquad (2)$$

In the first stage, physical bonded water and also in the upper part of the interval the coordinated water is lost (1). The existence of three water molecules coordinated at the central cation is sustained by the mass loss values recorded for each prepared complex. The activation energy is higher in case of yttrium compared with the lanthanides due its smaller ionic radius (0.93 Å compared to 1.04–1.00 Å). In the second stage, the percent of mass losses suggests the elimination of the pyridine ring due to the breaking of the covalent C–C bond between the two constituent rings of the ligand (Fig. 2). The process is sustained by the electromer effects occurring in the presence of the central cation and its coordinative bond established with the nitrogen atom in the pyridine ring. In the upper stages the decomposition processes evolves with further destructuration of the complexes accompanied by volatile exhaustions (2).

Besides the volatile products, a series of intermediate products like yttrium and lanthanide oxocarbonates[17] may occur (3) which further decomposes at more stable M_2O_3 products (4).[18, 19] The recorded mass of the residue for each prepared complex suggests the M_2O_3 as final decomposition product along with the presence of small amounts of residue resulted from decomposition of the ligand.

$$[(C_xH_yO_zN)_3M] \xrightarrow{300\text{–}650\,^\circ C} M_2O_2CO_3 + \text{volatiles} \qquad (3)$$

$$M_2O_2CO_3 \xrightarrow{650\text{–}1000\,^\circ C} M_2O_3 + \text{volatiles} \qquad (4)$$

IR Analysis

Investigation of the recorded IR spectra emphasized the interactions occurred between the ligand (HL) and the Y^{3+}, Eu^{3+}, Tb^{3+} cations. Figure 3 presents the recorded spectra for the free ligand and prepared complexes. The initial investigation of the free ligand was required to highlight the modifications occurred through complexation process. The recorded peaks of the functional groups specific to the free ligand were assigned as follows:[20, 21] 3445 cm^{-1}—$\boldsymbol{\nu}$N–H, 3144 cm^{-1}—$\boldsymbol{\nu}$N–H; 3086, 3066, 2932, 2862, 3144 cm^{-1}—$\boldsymbol{\nu}$C–H (pyridine and triazole ring); 1798 cm^{-1}—$\boldsymbol{\delta}^{\mathbf{ip}}$HNC; 1601 cm^{-1}—$\boldsymbol{\nu}$C=N (pyridine ring); 1562 cm^{-1}—$\boldsymbol{\nu}$C=C; 1477 cm^{-1}—$\boldsymbol{\nu}$C–N; 1435 cm^{-1}—$\boldsymbol{\delta}^{\mathbf{ip}}$C–H; 1400 cm^{-1}—$\boldsymbol{\nu}$C=N (both rings); 1323, 1204 cm^{-1}—$\boldsymbol{\delta}$C–H methylene, 1269, 1099 cm^{-1}—$\boldsymbol{\nu}$C–N (both rings); 1053 cm^{-1}—$\boldsymbol{\nu}$N–N (triazole ring); 1003 cm^{-1}—planar deformation pyridine ring; 903, 752 cm^{-1}—$\boldsymbol{\delta}^{\mathbf{oop}}$C–H; 802 cm^{-1}—$\boldsymbol{\delta}^{\mathbf{oop}}$C–N; 714 cm^{-1}—$\boldsymbol{\gamma}$ (triazole ring) and $\boldsymbol{\gamma}$CN; 667 cm^{-1}—$\boldsymbol{\gamma}$ (triazole ring) and $\boldsymbol{\gamma}$NH; 625 cm^{-1}—$\boldsymbol{\gamma}$ (triazole ring); 505 cm^{-1}—$\boldsymbol{\delta}^{\mathbf{oop}}$N–H; 467 cm^{-1}—non-planar pyridine ring deformation. (*where* $\boldsymbol{\nu}$*—stretching*, $\boldsymbol{\delta}$*—deformation*, **ip***—in plane*, **oop***—out of plane*, $\boldsymbol{\gamma}$*—out of plane bending*).

Table I. Chemical analysis experimental results compared with calculated values.

	Experimental values %				Calculated values %				
Prepared complex	C	H	N	O	M	C	H	N	O
$[YL_3(H_2O)_3]$	43.48	4.20	30.45	9.07	15.37	43.61	3.66	29.06	8.3
$[EuL_3(H_2O)_3]$	39.09	3.51	25.74	8.21	23.69	39.32	3.3	26.2	7.48
$[TbL_3(H_2O)_3]$	38.71	3.45	25.8	7.76	24.51	38.9	3.26	25.92	7.40

Table II. Kinetic parameters in thermal decomposition recorded for free complexes.

Decomposition stage	Parameter	$[YL_3(H_2O)_3]$	$[EuL_3(H_2O)_3]$	$[TbL_3(H_2O)_3]$
Stage 1	Pre-exponential factor	$7.6 \cdot 10^{15}$	$2.5 \cdot 10^{14}$	$2.8 \cdot 10^{15}$
	Activation energy (kJ/mol)	62.3	47.89	48.07
	Reaction order	0.68	1.61	1.03
	Temp. interval (°C)	91–156	78–155	80–144
	% loss	11.7/[a]9.33	10.93/[a]8.41	11.2/[a]8.32
Stage 2	Pre-exponential factor	$1.77 \cdot 10^{17}$	$6.26 \cdot 10^{14}$	$5.59 \cdot 10^{18}$
	Activation energy (kJ/mol)	72.8	68.10	59.13
	Reaction order	0.71	0.48	0.69
	Temp. interval (°C)	220–336	249–449	229–481
	% loss	36.25	34.5	34.12
Stage 3	Pre-exponential factor	$3.15 \cdot 10^{18}$	$3.35 \cdot 10^{17}$	$8.62 \cdot 10^{14}$
	Activation energy (kJ/mol)	52.07	45.72	73.99
	Reaction order	0.81	0.28	0.69
	Temp. interval (°C)	349–464	510–648	550–756
	% loss	11.19	25.52	25.02
Stage 4	Pre-exponential factor	$2.57 \cdot 10^{16}$	–	–
	Activation energy (kJ/mol)	63.8	–	–
	Reaction order	0.52	–	–
	Temp. interval (°C)	500–851	–	–
	% loss	20.67	–	–
Residue %		20.2/[b]19.52	29.07/[b]27,28	29.65/[b]28.07

Notes: [a]Calculated value for the presence of three water molecules coordinated at the central atom; [b]Calculated value for the final M_2O_3 decomposition product; M = Y^{3+}, Eu^{3+}, Tb^{3+}.

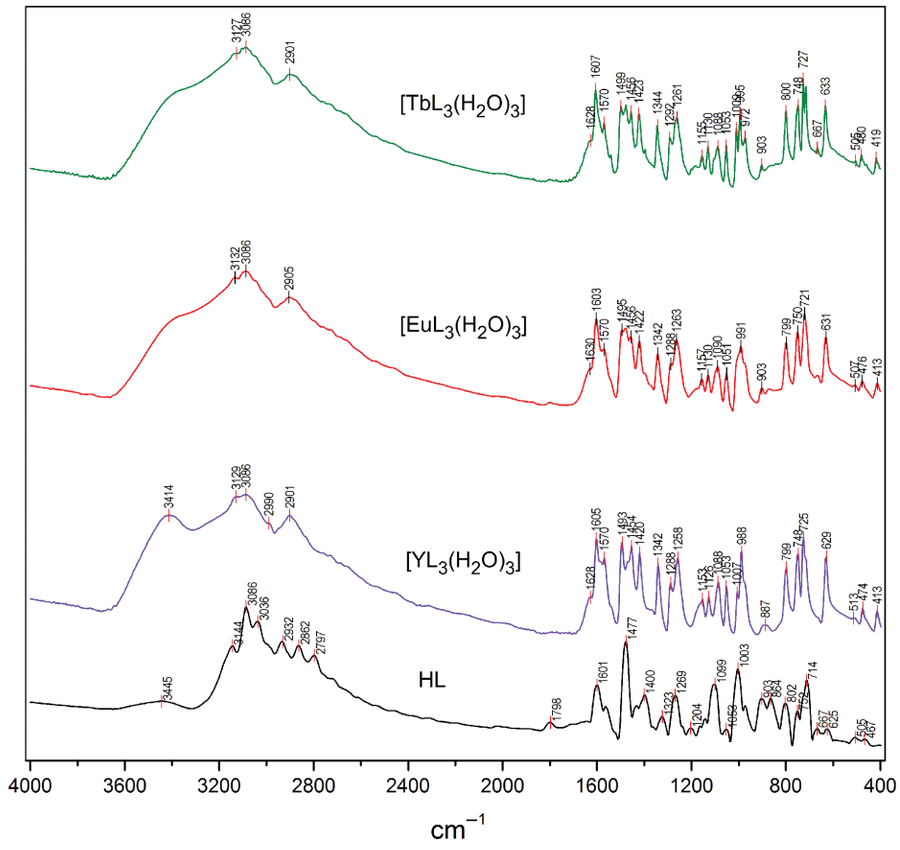

Figure 3. Recorded spectra for the free ligand and prepared complexes.

For a better view, in Table III are presented a series of significant changes occurred through complexation process. Besides the shifting of various peaks due to the rearrangements of various groups, through complexation a series of peaks as –NH specific stretching or deformation vibrations recorded in case of free ligand are no more present in the spectra of prepared complexes while new absorption peaks appear due to the establishment of the covalent bonds between the central trivalent cation and nitrogen atom from the former –NH group located in the triazole ring of the free ligand. These new established covalent bonds are sustained by the presence of new moderate intensity peaks located in the 403, 409, 419 cm^{-1},[22] while in case of the free ligand these peaks are absent. The νC=N in the pyridine ring which occurs at 1601 cm^{-1} in the free ligand, appear displaced in case of all prepared complexes due to the involvement in coordinative bonding with the central cation.

These new established bonds (coordinative and covalent) also triggers further planar or non-planar deformation of the pyridine ring which also tend to be displaced to higher wavenumbers (991, 991, 995 and 474, 476, 480 cm^{-1}) due to decreasing of the ionic radii leading to a higher ionic strength. The skeletal vibrations like stretching or bending of CH groups located both in pyridine and triazole rings are also influenced through complexation some of their specific peaks being broaden and slightly displaced. The diffuse broadening accompanied by the increasing of absorption intensity in the upper region of the spectra (3600–3000 cm^{-1}) is attributed of the presence of various types of water in the structure of the complexes.

The results confirm the proposed structure of the complexes (Fig. 1) through the bidentate behavior of the 2-(1H-1,2,4-Triazol-3-yl)pyridine ligand, the presence of coordinated water in the structure of the prepared complexes being in accordance with the results provided through chemical analysis and thermal behavior investigations.

Table III. Significant changes occurred through complexation process.

Functional group/ assignment	HL	$[YL_3(H_2O)_3]$	$[EuL_3(H_2O)_3]$	$[TbL_3(H_2O)_3]$
	(cm^{-1})			
δ^{ip}HNC	1798	–	–	–
γNH	667	–	–	–
δ^{oop}N–H	505	–	–	–
νM–N	–	409	413	419
νC=N (pyridine ring)	1601	1601	1603	1607
Non-planar pyridine ring def.	467	474	476	480
Planar pyridine ring def.	1003	988	991	99

Fluorescence Spectroscopy

The optical properties of the hydrogel composites rely exclusively on the photoluminescent properties of the embedded complexes. The radiative transitions responsible

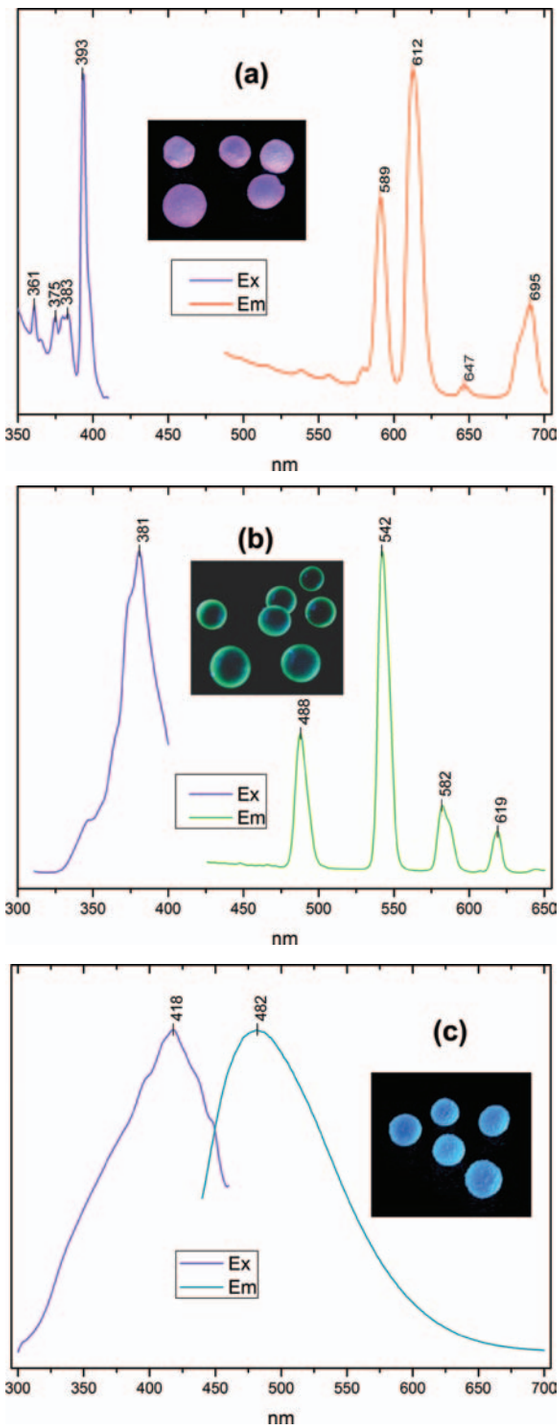

Figure 4. Excitation/emission spectra of hydrogel composites containing (a) $[EuL_3(H_2O)_3]$, (b) $[TbL_3(H_2O)_3]$ and (c) $[YL_3(H_2O)_3]$ complexes.

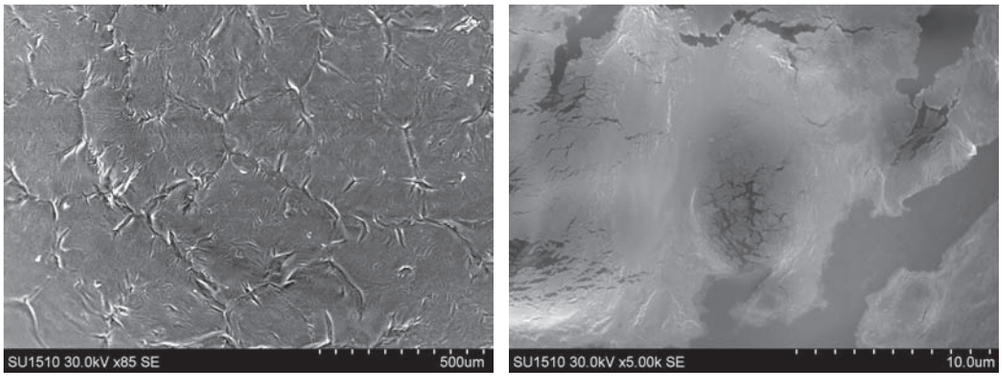

Figure 5. SEM images recorded for prepared hydrogel composite containing $[TbL_3(H_2O)_3]$ at 85× and 5000× magnifications.

for this property are based on different mechanisms and may be divided into two main categories. For the $[EuL_3(H_2O)_3]$ and $[TbL_3(H_2O)_3]$ complexes, characteristic metal centered, narrow emission bands arising from inner transitions within $4f$ orbitals are observed while in case of $[YL_3(H_2O)_3]$ complex the luminescence is rather a result of influence of the heavy cation vicinity (Y^{3+}) over the excited states of the ligand.

In case of $[EuL_3(H_2O)_3]$ and $[TbL_3(H_2O)_3]$ complexes, the chemical structure of the ligand and also the configuration achieved through complexation sustain the efficient sensitization of the Eu^{3+} and Tb^{3+} cations due to an indirect sensitization through the "antenna effect"[1] of the pyridine ring coupled to the triazole ring coordination site which subsequently transfers its excited states to the covalently bonded trivalent cation. The efficient sensitization process may be further aided by the presence of the coordinative bond between the nitrogen in the pyridine ring with the trivalent lanthanide cation. In Figures 4(a)–(c) are presented recorded and excitation spectra of the prepared hydrogel composites which are essentially similar to those recorded in case of corresponding free complexes. The only difference is noted in the intensities of the peaks which in case of hydrogel composites are slightly lower due to the reduced transparency of the polymer matrix.

The hydrogel composite containing $[EuL_3(H_2O)_3]$ complex (Fig. 4(a)) presents the most significant emission peaks located at 589 and 612 nm due to the $^5D_0 \rightarrow {}^7F_1$ and $^5D_0 \rightarrow {}^7F_2$ transitions. The barely observable peak located at 647 nm is due to the $^5D_0 \rightarrow {}^7F_3$ transition while the medium intensity peak centered at 695 nm is attributed to the $^5D_0 \rightarrow {}^7F_4$ radiative transition.[23] All the excitation peaks were recorded in the UV-A region, with the most intense peak located at 393 nm.

As for the $[TbL_3(H_2O)_3]$ contained hydrogel composite (Fig. 4(b)) same metal centered radiative transitions occurring within $4f$ orbitals were recorded, with the most intense emission peak located at 542 nm due to $^5D_4 \rightarrow {}^7F_5$ transition and a medium intensity peak recorded at 488 nm attributed to the $^5D_4 \rightarrow {}^7F_6$ transition. The less intense 582 nm peak is due to the $^5D_4 \rightarrow {}^7F_4$ transition while the lowest intensity 619 nm peak is assigned to the $^5D_4 \rightarrow {}^7F_3$ radiative transition.[23] The recorded excitation spectra revealed an intense broader peak centered around 381 nm.

For the case of hydrogel composite containing the $[YL_3(H_2O)_3]$ complex (Fig. 4(c)) the situation is different since the luminescence is a result of influence of the heavy cation vicinity (Y^{3+}) over the excited states of the ligand.[24] In its case, there is just one intense emission peak centered at 482 nm, significantly broader compared with the lanthanide prepared complexes. The recorded excitation spectra also revealed a wider peak, this time located in the upper region of the visible spectrum, at 418 nm.

Scanning Electron Microscopy (SEM)

Figure 5 shows microphotographs of the prepared hydrogel composite containing $[TbL_3(H_2O)_3]$ at two different resolutions. Both images show a relatively compact morphology with no evidence of complexes located at the surface of the hydrogel composites. The $[TbL_3(H_2O)_3]$ complex seems to be trapped within the polymer matrix.

CONCLUSIONS

The paper reports the obtaining and investigation of new photoluminescent hydrogel composites in which Y(III), Eu(III) and Tb(III) complexes with 2-(1H-1,2,4-Triazol-3-yl)pyridine as ligand are trapped in spherical shaped poly(acrylamide-co-acrylic acid) potassium salt beads. It was found that the addition of small amounts of glycerol provides long term dimensional stabilization of the hydrogel composites along with preservation of photoluminescent properties of the trapped complexes. Prior to embedment, the chemical structure of complexes was confirmed by elemental, thermal and FT-IR analyses. The photoluminescent properties of the resulting red, green and blue emitting hydrogel composites were investigated through fluorescence spectroscopy which revealed the most significant peaks located at 612, 542 and 482 nm while the excitation wavelengths are located in the UV-A region for the hydrogel composites containing the Eu(III)

and Tb(III) complexes and in the upper region of the visible spectrum for hydrogel composites containing the Y(III) complex.

Acknowledgments: This work was supported by a grant of the Romanian National Authority for Scientific Research, CNCS—UEFISCDI, project number PN-II-ID-PCE 2011-3-0708.

REFERENCES

1. S. A. Cotton, Lanthanide and Actinide Chemistry, edited by, Wiley & Sons **(2006)**.
2. L. Armelao, S. Quici, F. Barigelletti, G. Accorsi, G. Bottaro, M. Cavazzini, and E. Tondello, *Coord. Chem. Reviews* 254, 487 **(2010)**.
3. S. Petricek, *Acta Chim. Slov.* 56, 426 **(2009)**.
4. J. P. Leonard and T. Gunnlaugsson, *J. Fluorescence* 15, 585 **(2005)**.
5. K. Lunstroot, K. Driesen, P. Nockemann, K. Van Hecke, and L. Van Meervelt, *Dalton Trans.* 14, 298 **(2009)**.
6. C. S. Stan, I. Roşca, D. Sutiman, and M. S. Secula, *J. Rare Earths* 30, 401 **(2012)**.
7. C. S. Stan, M. Popa, and M. S. Secula, *J. Optical Materials* 35, 1741 **(2013)**.
8. M. Koppe, H. Neugebauer, and N. S. Sariciftci, *Mol. Cryst. Liq. Cryst.* 385, 221 **(2002)**.
9. L. G. Griffith, *Acta Mater.* 48, 263 **(2000)**.
10. F. Rossi, M. Santoro, T. Casalini, and G. Perale, *J. Rare Earth* 29, 259 **(2011)**.
11. C. Tan and Q. Wang, *Inorg. Chem.* 50, 2953 **(2011)**.
12. Z. Zhou and Q. Wang, *Sensors and Actuators*: *B. Chemical* 173, 833 **(2012)**.
13. T. Kowall, F. Foglia, L. Helm, and A. E. Merbach, *J. Am. Chem. Soc.* 117, 3790 **(1995)**.
14. Z. Ahmed and K. Iftikhar, *Inorg. Chem.* 13, 1253 **(2010)**.
15. G. S. Kottas, M. Mehlstubl, R. Fröhlich, and L. De Cola, *Eur. J. Inorg. Chem.* 22, 3465 **(2007)**.
16. A. Kumar, B. K. Sinha, G. Prasad, R. Kant, and S. Kumar, *Asian J. Chemistry* 12, 335 **(2000)**.
17. A. Kula, *J. Therm. Anal. Calorim.* 75, 79 **(2004)**.
18. C. R. S. Morais, A. G. Souza, P. A. Santa-Cruz, *J. Alloys Compd.* 344, 101 **(2002)**.
19. J. J. Zhang, N. Ren, Y. X. Wang, S. L. Xu, R. F. Wang, and S. P. Wang, *J. Braz. Chem. Soc.* 17, 1355 **(2006)**.
20. F. Billes, H. Endredi, and G. Keresztury, *Journal of Molecular Structure* (*Theochem*) 530, 183 **(2000)**.
21. Y. Buyukmurat and S. Akyuz, *J. Mol. Struct.* 563–564, 545 **(2001)**.
22. K. Mohanan, M. Thankamony, and B. Sindhu Kumari, *J. Rare Earths* 26, 463 **(2008)**.
23. G. Liu and B. Jacquier, Spectroscopic Properties of Rare Earth in Optical Materials, Springer **(2005)**, ISBN: 3-540-23886-7.
24. Z.-H. Tang, D.-Y. Liu, Y. Tang, and X.-P. Cao, *J. Innorganic and General Chemistry* 634, 392 **(2008)**.